

# Effect of Caesium Based Compounds As Electron Injection Layer In Fluorescent Polymer Organic Light-Emitting Diode

Calvin Yi Bin Ng<sup>a</sup>, Kai Lin Woon<sup>a\*</sup>

<sup>a</sup>*Physics Department, Faculty of Science, Low Dimensional Material Research Centre (LDMRC),  
University of Malaya, 50603 Kuala Lumpur, Malaysia*

\* *E-mail: ph7klw76@um.edu.my*

**Abstract.** Electron transport in light emitting semiconducting polymers is often limited by traps. By studying the role of Caesium carbonate ( $\text{Cs}_2\text{CO}_3$ ), *Caesium Nitride* ( $\text{CsN}_3$ ), *Caesium Fluoride* ( $\text{CsF}$ ) are chosen as the electron injection layer, it is discovered that  $\text{CsF}$  has the ability to reduce the electron traps followed by  $\text{CsN}_3$  and then  $\text{Cs}_2\text{CO}_3$  with trap density of  $1.5 \times 10^{18} \text{ cm}^{-3}$ ,  $2.22 \times 10^{18} \text{ cm}^{-3}$ ,  $3.03 \times 10^{18} \text{ cm}^{-3}$ , respectively. We also found out that for such materials, charge balance as often obtained from comparison between electron and hole only devices, is not a good predictor for current efficiency. In fact, highest efficiency is obtained using  $\text{Cs}_2\text{CO}_3$  with 11.9 lm/W for superyellow poly-(p-phenylenevinylene) at  $1000 \text{ cdm}^{-2}$ .

**Keywords:** superyellow, Caesium, traps, polymer light emitting diodes

## INTRODUCTION

Organic light-emitting diodes (OLEDs) are penetrating the flat panel display markets thanks to the rapid progress in academia and industry research efforts. Charge balance in OLEDs is one of the critical parameters that determines the current efficiency of the device [1-3]. Achieving charge balance is one of the major focus of research. With electron and hole blocking layers, charge can be confined within the emissive layer resulting in remarkable improvement in vacuum-deposited small molecules OLEDs [4-6]. Applying these techniques in solution processable OLEDs are more challenging, despite of that progress has been made [7,8]. Despite of remarkable luminescence behavior of light emitting polymer, efficiency of polymer light emitting diodes (PLED) has been lagging behind that of small molecules OLEDs.

The electron transport in most semiconducting polymers is inferior to the hole transport [9]. These semiconducting polymers often show considerable lowered electron current than the hole current. One of the key requirements for an efficient light emitting diode is the charge balance. In order to overcome the trap-limited electron current of semiconducting polymers, novel methods are employed such as the use of polar solvents to induce a higher vacuum level shift [10, 11], diluting the light emitting polymer with higher band-gap hosts [12, 13] and trap-filling with 2,3,5,6-Tetrafluoro-2,5-cyclohexadiene-1,4-diylidene) dimalononitrile  $\text{F}_4\text{-TCNQ}$  [14]. Although these methods results in better device efficiency, there is no study of how electron injection layer (EIL) can affect the electron trap limited semiconducting polymers.

Often a low work function electrode is used, coupled with an efficient electron injection layer, in order to 'flood' the semiconducting polymers with electrons. Caesium based compounds are often used as an electron injection layers. These include Caesium quinine-8-oxide (Csq) [15], Caesium carbonate ( $\text{Cs}_2\text{CO}_3$ ) [16, 17], Caesium pivalate ( $\text{C}_5\text{H}_9\text{O}_2\text{Cs}$ ) [18], Caesium phosphate ( $\text{Cs}_3\text{O}_4\text{P}$ ) [19], Caesium fluoride (CsF) [20], just to name a few. The semiconducting polymer poly (*p*-phenylene vinylene) (PPV) and its derivatives have been used as model compounds to investigate the charge transport in polymer light emitting diodes (PLEDs). Here, we would like to study the effect of Caesium based compounds in yellow emitting poly-(*p*-phenylenevinylene) (SY-PPV). It was found charge balance, based on hole and electron only devices, is not a good predictor for current efficiency for such materials. By performing capacitance measurements, we found that the density of electron traps can be reduced by using CsF as an electron injector. High electron current can be achieved suggesting the possibility of trapping filling behavior of CsF.

## EXPERIMENTAL METHODS

The device consists of indium tin oxide (ITO) / poly (3,4-ethylenedioxythiophene):polystyrene sulfonate (PEDOT:PSS) / SY-PPV/ electron injection layer (1nm)/ Al (100 nm). Caesium carbonate ( $\text{Cs}_2\text{CO}_3$ ), Caesium Nitride ( $\text{CsN}_3$ ), Caesium Fluoride (CsF) are chosen as the EIL under this study. ITO substrates were cleaned using DI water, acetone, and isopropyl alcohol sequentially in the ultrasonic bath followed by oxygen plasma treatment with 35 W for 5 minutes. 40 nm PEDOT:PSS was then spin coated on top of ITO followed by annealing at 150 °C for 10 minutes in  $\text{N}_2$  environment. SY-PPY (PDY-132 from Merck) was then spin coated on top of PEDOT:PSS forming a 80 nm film followed by annealing at 100°C. Current-Voltage-Luminance (J-V-L) measurement of the PLED devices are carried out using Konica Minolta CS-320 Chroma-meter and Keithley 236 sourcemeter unit. The device is further characterized using Agilent 4294A impedance analyzer scanning with a range of frequency (C-f) or voltage (C-V).

## RESULTS AND DISCUSSIONS

Figure 1(a) and (b) shows the current density and luminance as a function of voltage. The device with  $\text{Cs}_2\text{CO}_3$  as a buffer layer shows the lowest current density across whole voltage range followed by  $\text{CsN}_3$  while CsF shows the highest current density. This indicates that the device with CsF as cathode EIL layer has a higher injection of electron density compared to the  $\text{Cs}_2\text{CO}_3$ . In terms of luminance, CsF shows the highest luminance across the full range of applied bias as shown in Figure 1(b) followed by  $\text{CsN}_3$ , and  $\text{Cs}_2\text{CO}_3$ . As the current density for CsF is the highest, more electrons were injected into the device and this increases the possibility of effective recombination. Therefore, it was expected that the luminance for CsF device showed the highest luminescence compared to  $\text{Cs}_2\text{CO}_3$ . Figure 1(c) and (d) show the power efficiency and current efficiency as a function of voltage. Regardless of higher current density and luminance achieved by CsF and  $\text{CsN}_3$  devices, the performance was in the opposite. Device with  $\text{Cs}_2\text{CO}_3$  shows the highest power efficiency followed by  $\text{CsN}_3$  and CsF. Furthermore, there is a huge difference in terms of performance between  $\text{Cs}_2\text{CO}_3$ , and  $\text{CsN}_3$ /CsF.

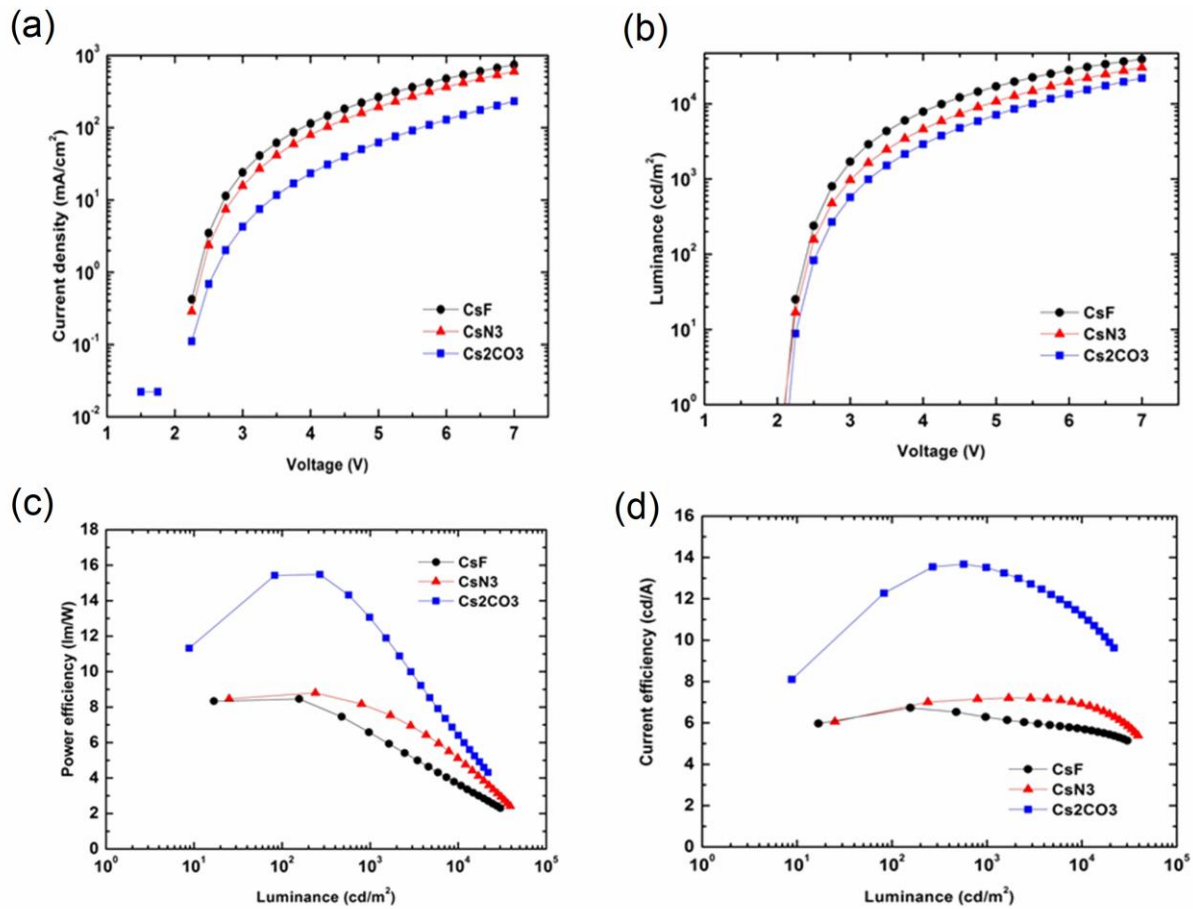


**FIGURE 1.** (a) Current density-voltage characteristics and (b) Luminance-voltage characteristics, (c) Power efficiency and (d) Current efficiency for PLED with Cs<sub>2</sub>CO<sub>3</sub>/CsF/CsN<sub>3</sub> as EIL for PLED with Cs<sub>2</sub>CO<sub>3</sub>/CsF/CsN<sub>3</sub> as EIL.

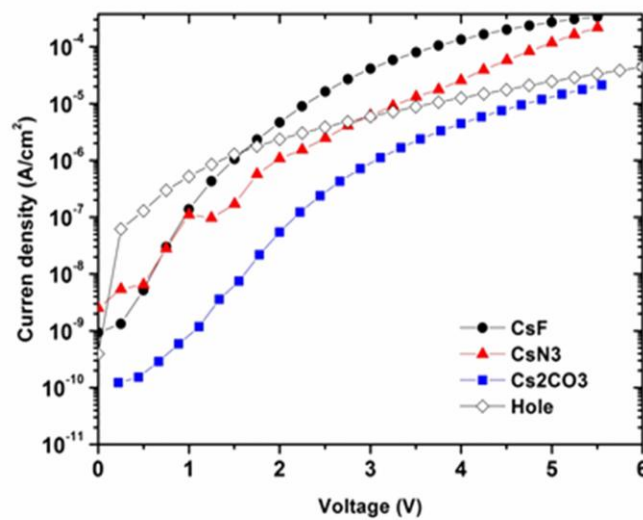


**FIGURE 2.** Electron and hole-dominated current density as a function of voltage for PLED with Cs<sub>2</sub>CO<sub>3</sub>/CsF/CsN<sub>3</sub> as EIL.

Since the modification was only done on the cathode, in order to study the transport properties of electron, electron-only devices for different Caesium based compounds were fabricated along with hole-only device. Figure 2 shows the electron and hole-only current density as a function of applied voltage. There are two points can be observed: First, the electron current for CsF device is the highest followed by CsN<sub>3</sub> and Cs<sub>2</sub>CO<sub>3</sub>. This means that the electron density injected from the cathode with CsF is the highest while the Cs<sub>2</sub>CO<sub>3</sub> has the lowest value. It can be observed that the electron current for CsN<sub>3</sub> is closer to hole current compared to Cs<sub>2</sub>CO<sub>3</sub> and CsF. However, device with high electron current and charge balancing observed for CsF and CsN<sub>3</sub>, respectively, have a poorer efficiency than Cs<sub>2</sub>CO<sub>3</sub>, the device with a low electron current. This provided some important clue to understand the underlying mechanism involved. In fact, high electron density does not guarantee a high device efficiency as the electron current is originated from how many electrons were collected at the anode. More electrons collected from the anode means that the zone of recombination might be shifted near to the anode. Higher value of electron current can be also due to fewer electrons trapping effect. Therefore, traps affect the magnitude of electron current and recombination zone which eventually determines the device efficiency. Even the electron current is identical to the hole current, the recombination zone might be very near to the anode where quenching of excitons is prone to happen. In this case, the use electron only device might not be a good choice to explain charge balance. Due to this, the device performance of CsN<sub>3</sub> device did not show better efficiency than Cs<sub>2</sub>CO<sub>3</sub> even with its electron current almost identical to the hole current.

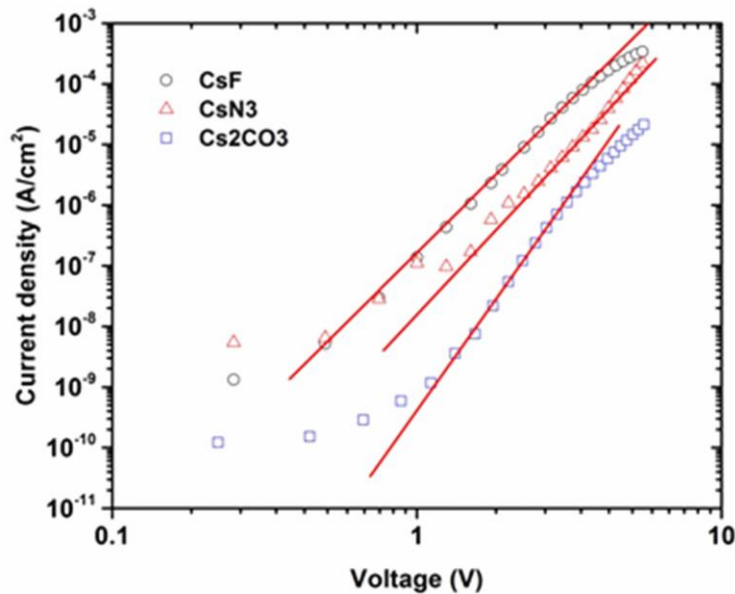


**FIGURE 3.** Log-log plot of current density and voltage for electron-only devices. The red-lines were obtained by fitting the experimental data with a power law.

For electron injection, the trap-filled limited current density  $J_{TCL}$  can be expressed as [21]

$$J_{TCL} = N_{LUMO} \mu_n q^{(1-m)} \left( \frac{\epsilon m}{N_T(m+1)} \right)^m \left( \frac{2m+1}{m+1} \right)^{(m+1)} \frac{V^{(m+1)}}{d^{(2m+1)}} , \tag{1}$$

where  $m = T_t/T$ ,  $d$  is polymer film thickness,  $\mu_n$  is the electron mobility,  $N_{LUMO}$  is the density of states in LUMO level,  $V$  is the applied voltage,  $\epsilon$  is the permittivity,  $N_T$  is the charge trap density and  $q$  is the electronic charge. Hence, the filling up the empty traps results in rapid increase in current density according to this power law ( $J \propto V^{(m+1)}$ ). In Figure 3, slopes were obtained by fitting the experimental data using power law.

In order to further study the transport properties of electron, a log-log plot of current density and voltage for all the electron-only devices is shown in Figure 3. It is known that the use of Caesium based compounds as EIL by thermal deposition method can introduce new energy levels at the band-gap (traps) in the organic layer underneath [8]. The occurrence of abruptly increase of the electron current at certain voltage is the characteristics for insulator with trap states [9] which can be observed for all electron current in Figure 3. This J-V characteristic region where the sharp transition occurred in Figure 3 is well described by Equation 1 which is the trap-filled limited current. Assuming  $N_{LUMO} = 2.5 \times 10^{19} \text{ cm}^{-3}$  [9] and  $\mu_n$  is constant, it follows from Equation 1 that  $N_T = 1.5 \times 10^{18} \text{ cm}^{-3}$  for CsF,  $2.2 \times 10^{18} \text{ cm}^{-3}$  for CsN<sub>3</sub> and  $3.0 \times 10^{18} \text{ cm}^{-3}$  for Cs<sub>2</sub>CO<sub>3</sub>. Using these parameters, we find a good agreement between the experimental and theoretical results at TCL regime in Figure 3. Thus, this confirms that electron current is limited by the presence of trap states; the higher the density of trap states, the lower the electron current becomes. Moreover, knowing the traps energy level is fairly important as well. Estimation of depth for trap energy level was proposed to be related to the slope of J-V in the log-log plot [9]. The depth of trap can be estimated by fitting power law from the slope of the curve in Figure 3. The slopes obtained were  $5.21 \pm 0.02$  for CsF,  $6.85 \pm 0.08$  for CsN<sub>3</sub> and  $7.52 \pm 0.09$  for Cs<sub>2</sub>CO<sub>3</sub>. It is known that both CsF and CsN<sub>3</sub> could decompose during thermal deposition and generate Cs while Cs<sub>2</sub>CO<sub>3</sub> could partially decompose with the product of CsO<sub>2</sub> [22].

The product of the decomposition could induce gap states between LUMO and HOMO. With the information extracted from the electron current, an explanation for the origin of the difference of device's performance is proposed. When CsF, CsN<sub>3</sub> and Cs<sub>2</sub>CO<sub>3</sub> were used as EIL, trap states were introduced in the polymer. As electrons were injected, trap states were being filled up and followed by de-trapping. Hence, the amount of trap states and its depth determine the electron current. From Figure 3, the device with CsF as EIL has the shallowest traps and lowest amount of trap states while the Cs<sub>2</sub>CO<sub>3</sub> has the deepest and highest amount of trap states. This indicates that the electrons for device with Cs<sub>2</sub>CO<sub>3</sub> were severely limited by the large number of deep traps as compared to CsF and CsN<sub>3</sub>. On the other hand, CsF and CsN<sub>3</sub> have fewer and shallower traps which means the transfer rate for electron is enhanced, which results in higher electron current. However, due to high electron current, recombination is prone to happen near the anode. Hence, exciton quenching effect at the anode could be one of the reasons for poor performance of these two devices. In order to investigate this hypothesis, capacitance-frequency/voltage measurements were carried out to investigate the effects of these EILs on electron current.

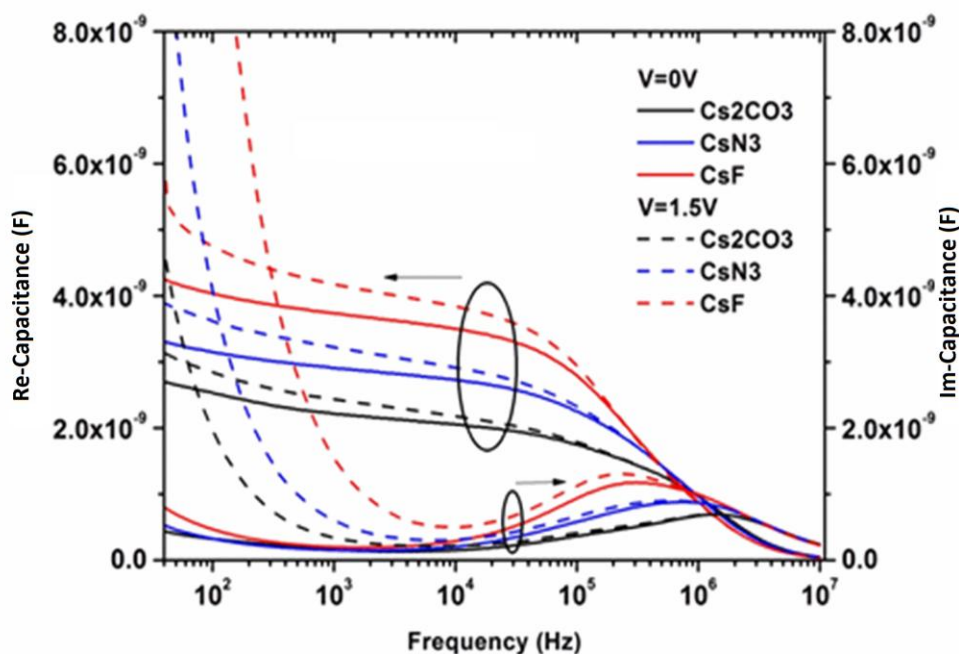


**FIGURE 4.** Real part and imaginary part of capacitance spectra measured at 0.0V and 1.5V DC bias with 0.5V AC bias for device with different EILs.

A Polymer LED can be regarded as a capacitor where a dielectric layer was sandwiched between electrodes. At a constant external voltage, as compared to a capacitor in vacuum, the introduction of a dielectric into a capacitor increases the storage capacity as more charge flows into it. The increased capacitance is due to the polarization of dielectric as the positive and negative charges within it are displaced slightly from their normal position. The polarization mentioned here acts in the same way as a field in capacitor. Any possible changes on the polarization due to doping or traps can be detected from its capacitance. As shown in Figure 4, an increase of capacitance at low-frequencies due to the mobile charge carriers can be observed. In polymer materials, there are two kinds of charge carriers, hole (electron) and ion where the latter could be the residuals elements originated from material synthesizing process or due to the decomposition of Caesium based compounds. Therefore, the trap states as mentioned before could be electron trap or ionic trap. If an external bias was applied, electrons or ions moves by hopping towards the electrode and accumulated. As a result, an additional capacitance was created and the real-part of low-frequencies capacitance was affected. However, the accumulation of ions does not affect the frequency-dependent imaginary part of capacitance which is related to imaginary part of dielectric constant as the accumulated charges are static. Therefore, this strongly suggests that the charge carriers contributed to the capacitance are electrons instead of ions as the imaginary part of dielectric due to ionic impurity would be frequency-dependent. Furthermore, the capacitance at low-frequencies region was the highest for CsF followed by CsN<sub>3</sub> and Cs<sub>2</sub>CO<sub>3</sub> at zero bias. This trend was found to be consistent with J-V plot for electron-only device which indicates that the extra charge carriers were induced inside the device. As there is no modification being done on anode, it is strongly suggests that the changes of capacitance at zero bias is due to cathode modification by Caesium based compounds.

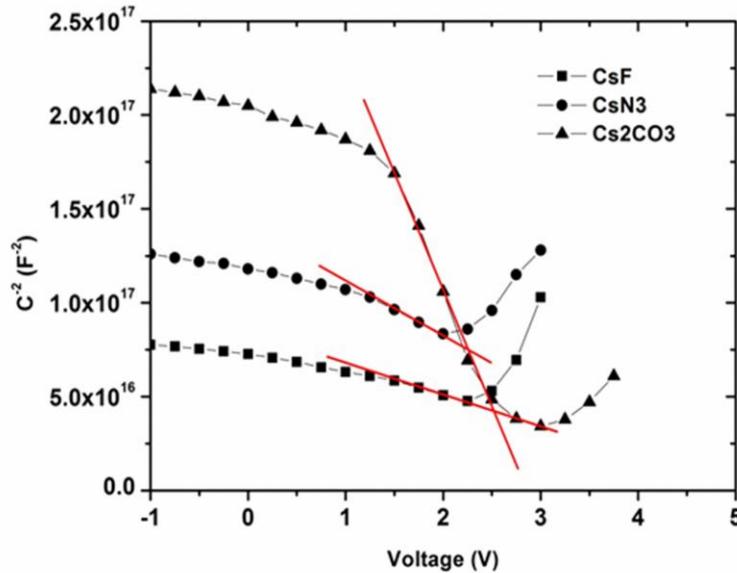
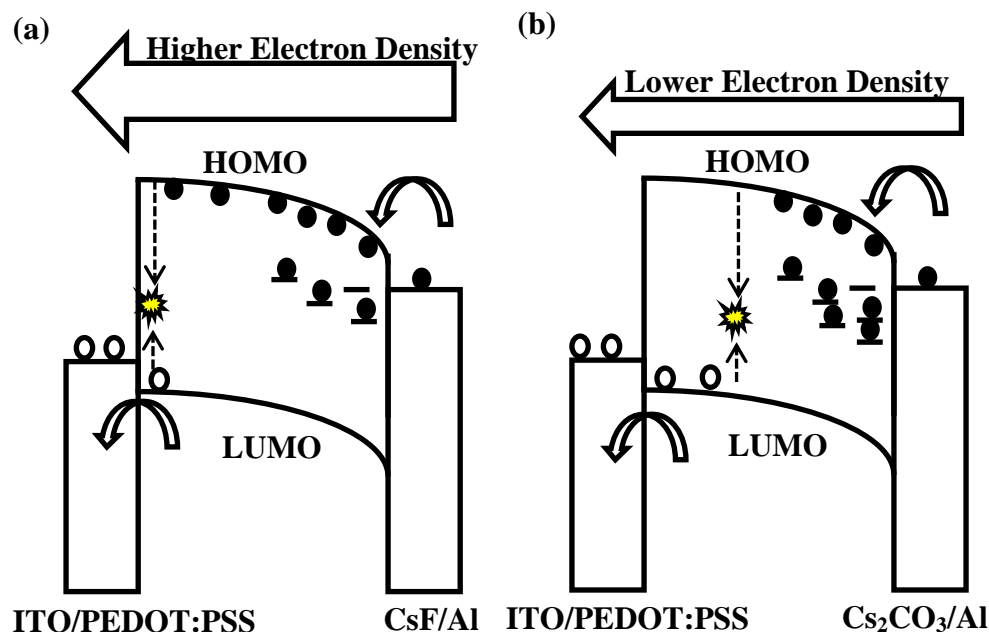


FIGURE 5. Mott-Schottky plot for device with different EILs. The red-lines are intended to guide the eye.

It is known that the introduction of Caesium based compounds can lead to n-doping of the organic material [23]. The dopant density,  $N_A$  can be estimated by using Mott-Schottky plot as shown in Figure 5 and it is described by:

$$\frac{1}{C^2} = \frac{2(V_{bi}-V)}{q\epsilon_r\epsilon_0A^2N_A}, \tag{2}$$

where  $C$  is the capacitance,  $V_{bi}$  is the built-in potential,  $\epsilon_r$  and  $\epsilon_0$  are the dielectric constant for organic layer and vacuum permittivity,  $A$  is the device area and  $N_A$  is the doping density. The doping density,  $N_A$  can be extracted from the linearity of  $C^{-2}$  vs  $V$ . The linearity was shown in Figure 5 by red lines. The doping density,  $N_A$  obtained for Cs<sub>2</sub>CO<sub>3</sub> is  $1.74 \times 10^{17} \text{ cm}^{-3}$ , CsN<sub>3</sub> is  $8.89 \times 10^{17} \text{ cm}^{-3}$  and  $1.58 \times 10^{18} \text{ cm}^{-3}$  for CsF. From this result, doping density for CsN<sub>3</sub> and CsF was apparently higher than Cs<sub>2</sub>CO<sub>3</sub>. This strongly suggests that more negative charges were introduced (n-doped) after the insertion of CsN<sub>3</sub> and CsF as compared to Cs<sub>2</sub>CO<sub>3</sub>. This leads to a higher capacitance at zero bias for CsF and CsN<sub>3</sub> as compared to Cs<sub>2</sub>CO<sub>3</sub>.



**FIGURE 6.** Energy diagram shows the working mechanism for PLED with (a) CsF and (b) Cs<sub>2</sub>CO<sub>3</sub> as the electron injection layer.

**TABLE 1.** Summary for the trend of each parameter for different Caesium based compounds. Power efficiency is obtained at 1000 cdm<sup>-2</sup>

Caesium based compounds	Doping density (cm <sup>-3</sup> )	Capacitance at zero bias (nF)	Trap density, (cm <sup>-3</sup> )	Electron Current density (Acm <sup>-2</sup> )	Power Efficiency (lm/W)
CsF	Highest 1.58 x 10 <sup>18</sup>	Highest 3.72	Lowest 1.15 x 10 <sup>18</sup>	Highest 4.09 x 10 <sup>-5</sup>	Lowest 5.93
CsN <sub>3</sub>	Medium 8.89 x 10 <sup>17</sup>	Medium 2.91	Medium 2.22 x 10 <sup>18</sup>	Medium 6.17 x 10 <sup>-6</sup>	Medium 7.54
Cs <sub>2</sub> CO <sub>3</sub>	Lowest 1.74 x 10 <sup>17</sup>	Lowest 2.22	Highest 3.03 x 10 <sup>18</sup>	Lowest 1.12 x 10 <sup>-7</sup>	Highest 11.89

Caesium based compounds were known to introduce trap states in an organic layer after thermal deposition. Different compounds show different amount of trap states as well as different n-doping capability as supported by the Mott-Schottky plot. The device with the highest doping density has the lowest density of traps while the device with the lowest doping density has the highest density of traps as shown in Table 1. A possible mechanism behind the different performances with different EILs can be proposed. For device with CsF, the trap states is the lowest in density as the doping density is the highest. Due to this, the charge density was the highest at zero bias as shown by the geometric capacitance. When voltage increases, electrons



are injected and trap-filling occurs. For CsF, the electron current is less limited by traps. As a result, the electron current increases and the zone of recombination is shifted towards anode which increases the probability of exciton quenching as shown in Figure 6. On the other hand, Cs<sub>2</sub>CO<sub>3</sub> has the greatest number of traps as the doping density is the lowest. Therefore, the electron current is lower. However, this helps to reduce the probability of exciton quenching at the anode as the zone of recombination was further away from the anode. The device with Cs<sub>2</sub>CO<sub>3</sub> exhibits better charge balance as compared to CsF and CsN<sub>3</sub>. This results in higher efficiency of polymer LEDs. Furthermore, Cs<sub>2</sub>CO<sub>3</sub> was known to be more stable than CsF and CsN<sub>3</sub> which were very sensitive to moisture and oxygen. Moreover, the decomposition of CsF and CsN<sub>3</sub> was known to be containing Cs metal which could cause quenching effect [24]. So, these two factors could also be one of the possible contributions to the low device efficiency of CsF and CsN<sub>3</sub>.

## CONCLUSIONS

The charge balance as obtained from the electron and hole only devices are not good predictor for current efficiency for electron trap limited light emitting polymer such as super yellow polymer. The electron traps can be reduced by CsF, resulting in electron flooding into the device as a result of trap filling by n-doping. However, the highest efficiency of super yellow device is obtained when Cs<sub>2</sub>CO<sub>3</sub> as an electron injection layer is used, which has the least doping effect as compared with CsF and CsN<sub>3</sub>.

## ACKNOWLEDGMENTS

This research was supported by the University of Malaya UMRG Grant (RP026A-15AFR) and Ministry of Science, Technology and Innovation (MOSTI) Malaysia (SF019-2014) and ItraMAS Technology for partial Funding.

## REFERENCES

1. D.C. Huang, Y.L. Chen, K.Y. Wu, Y.T. Tao, *Langmuir*, **28**, 424–430 (2012)
2. X. Xing, L. Zhang, R. Liu, S. Li, B. Qu, Z. Chen, W. Sun, L. Xiao, Q. Gong, *ACS Appl. Mater. Interfaces*, **4**, 2877–2880 (2012)
3. S. Y. Kim, K. Honga, H. W. Choi, K. Y. Kim, Y.H. Tak, J.L. Lee, *J. Electrochem. Soc.* **156**, J57-J61 (2009)
4. H. Kuma, Y. Jinde, M. Kawamura, H. Yamamoto, T. Arakane, K. Fukuoka, C. Hosokawa, *SID Int. Symp. Dig. Tec. part1-2*, **38**, 1504-1507 (2007)
5. Y. Seino, S. Inomata, H. Sasabe, Y. J. Pu, J. Kido, *Adv. Mater.* **28**, 2638–2643 (2016)
6. M. G. Helander, Z. B. Wang, J. Qiu, M. T. Greiner, D. P. Puzzo, Z. W. Liu, Z. H. Lu, *Science* **332**, 944-7 (2011)
7. Z. A. Hasan, K. L. Woon, W. S. Wong, A. Ariffin, S. A., *J. Lumin.* **183**, 150–158 (2017)
8. S. Wang, B. Zhang, Y. Wang, J. Ding, Z. Xie, L. Wang, *Chem. Commun.*, **53**, 5128-5131 (2017)
9. H. T. Nicolai, M. Kuik, G. A. H. Wetzelaer, B. de Boer, C. Campbell, C. Risko, J. L. Brédas, P. W. M. Blom, *Nat. Mater.* **11**, 882–887 (2012)

10. C. Y. B. Ng, K. H. Yeoh, T. J. Witcher, N. A. Talik, K. L. Woon, T. Saisopa, H. Nakajima, R. Supruangnet, P. Songsiriritthigul, *J. Phys. D: Appl. Phys.* **47**, 015106 (2014)
11. Q. Q. Song, C. Song, Z. M. Zhong, Z. H. Hu, L. Wang, J. Wang, Y. Cao, *Org. Electron.* **24**, 241-245 (2015)
12. D. Abbaszadeh, P.W.M. Blom, *Adv. Electron. Mater.* **2**, 1500406 (2016)
13. D. Abbaszadeh, A. Kunz, G. A. H. Wetzelaer, J. J. Michels, N. I. Crăciun, K. Koynov, I. Lieberwirth, P. W. M. Blom, *Nat. Mater.* **15**, 628–633 (2016)
14. G. Zuo, Z. Li, O. Andersson, H. Abdalla, E. Wang, M. Kemerink *J. Phys. Chem. C* **121**, 7767–7775 (2017)
15. K. Xie, J. Qiaoa, L. Duan, Yang Li, Deqiang Zhang, Guifang Dong, Liduo Wang, and Yong Qiub *Appl. Phys. Lett.* **93**, 183302 (2008)
16. M.H Chen, I. Chih Wu, *Appl. Phys. Lett.* **104**, 113713 (2008)
17. R. Suhonen, R. Krause, F. Kozłowski, W. Sarfert, R. Patzold, A. Winnacker, *Org. Electron.*, **10**, 280-288 (2009)
18. S. Ronggang, G. Mu, X. Qiao, L. Wang, K. W. Cheah, X. Zhu, C. H. Chen. *Org. Electron.* **12**, 1957-1962, (2011)
19. J. H. Wemken, R. Krause, T. Mikolajick, G. Schmid *J. Appl. Phys.* **111**, 074502 (2012)
20. Huai-Xin Wei., Qing-Dong Ou, Zheng Zhang, Jian Li, Yan-Qing Li, Shuit-Tong Lee, Jian-Xin Tang, *Org. Electron.* **14**, 839–844 (2013)
21. Blom, P.W.M, de Jong, M.J.M , Vleggar, J.J.M, *Appl. Phys. Lett.* **68**, 3308-3310 (1996)
22. J. Huang, Z.Xu, Y. *Advanced Functional Materials* **17**, 1966–1973 (2007)
23. Y. H. Deng, Y.Q. Li, Q. D. Ou, Q. K. Wang, F. Z. Sun, X. Y. Chen, J. X. Tang, *Org. Electron.*, **15**, 1215-12 (2014)
24. V. van Elsbergen, C. Weijtens, J. Zaumseil, *Appl. Surf. Sci.*, **234**, 120-125 (2004)